European **J**ournal of **Chem**istry

Antimicrobial and catalytic applications of TiO$_2$ nanoparticles prepared from titanium(IV)-Schiff base complexes as precursor

Mohammad Nasir Uddin [iD] [1],*, Tareq Mahmud [iD] [1], Wahhida Shumi [iD] [2] and AKM Atique Ullah [iD] [3]

[1] *Department of Chemistry, Faculty of Science, University of Chittagong, Chattogram-4331, Bangladesh*
mnuchem@cu.ac.bd (M.N.U.), tareqromsony@gmail.com (T.M.)
[2] *Department of Microbiology, Faculty of Biological Science, University of Chittagong, Chattogram-4331, Bangladesh*
shumi@cu.ac.bd (W.S.)
[3] *Nanoscience and Technology Research Laboratory, Atomic Energy Centre, Bangladesh Atomic Energy Commission, Dhaka 1000, Bangladesh*
atique.chem@gmail.com (A.A.U.)

* *Corresponding author at: Department of Chemistry, Faculty of Science, University of Chittagong, Chattogram-4331, Bangladesh.*
 e-mail: mnuchem@cu.ac.bd (M.N. Uddin).

RESEARCH ARTICLE

ABSTRACT

Attempts have been made to synthesis titanium dioxide (TiO$_2$) nanoparticles using titanium (IV) complexes of Schiff base (TiOL) as a precursor where Schiff base ligand (L) act as a dibasic tetradentate one. TiO$_2$ nanoparticles were synthesized by the direct calcination of titanium complexes at 500 °C for 3 hours. The analytical tools such as FT-IR, XRD, EDS, and SEM provided evidences in favor of the formation of TiO$_2$ nanoparticles. Antimicrobial study showed that all prepared TiO$_2$ nanoparticles have inhibition capacity on the growth against selected plant pathogenic fungi as well as some selected human pathogenic bacteria. Moreover, these TiO$_2$ nanoparticles have catalytic capacity for the remarkable degradation (54.0%) of organic dye (Mordent brown 48) as well as industrial dye solutions.

Cite this: *Eur. J. Chem.* **2021**, *12(2)*, 124-132 | **Journal website**: www.eurjchem.com

1. Introduction

Condensation method is one of the best and easiest methods for the synthesis of Schiff bases from primary amine (-NH$_2$) and carbonyl compound (-C=O) under specific conditions [1]. Generally, Schiff bases are being used as ligands in coordination chemistry and exhibit a wide range of biological and chemical activities [2-5]. The chemistry of Schiff base complexes becomes popular and attractive to the researchers because of their salient features and simple synthesis methods. Moreover, these metal complexes can be used as catalysts, anticancer agents, antibacterial, antifungal, and cytotoxic agents [6,7]. Recently, Schiff base metal complexes are being used as a precursor for the synthesis of metal oxide nano-particles [8,9]. Because of the versatile activities, metal oxide nanoparticles are remarkable in various sectors. In addition, nanoparticles have recently been entered to commercial exploration period [10,11].
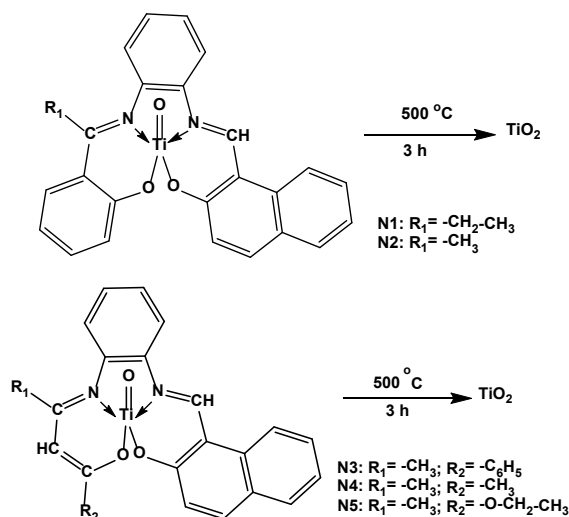
For the preparation of metal oxide nanoparticles, various substances were used as a precursor through different methods. Among all the techniques solid-state thermal decom-

position is better than any other method as it is economical, no use of toxic solvents, and much faster [12,13]. Earlier different metal oxide nanoparticles were synthesized from Schiff base metal complexes [8,9]. Hence, an attempt has been taken for the preparation of TiO$_2$ nanoparticles from titanium-Schiff base complexes which is not yet prepared from this source.

There are a number of applications of TiO$_2$ nanoparticles, i.e. photocatalytic activity to decompose organic dyes in waste water and as an antimicrobial agent. It is also used in surface modification such as coatings, in the production of self-cleaning materials, in light-emitting diodes and solar cells, in housing and construction for its UV absorption and photocatalytic properties and in sunscreens [14,15]. The pure nanosized TiO$_2$ has been produced after calcination of the titanium complexes of Schiff bases at 500 °C [16,17]. The produced nanosized TiO$_2$ was characterized by Fourier Transform infrared spectrometer (FTIR), X-ray diffraction (XRD), scanning electron microscope (SEM), and Energy-dispersive X-ray spectroscopy (EDS). The catalytic activity of the prepared TiO$_2$ NPs has been investigated by the degradation of organic dyes under sun light.

Table 1. The physical properties of the prepared Schiff base complexes as used for TiO_2 nanoparticle synthesis, their identification, and characteristic infrared frequencies (cm^{-1}).

Complexes	Identification code	R_1	R_2	Color	Melting point (°C)	Yield (%)	NPs	FTIR, vTi-O
TiO (HNP-OPD-HPP)	N1	CH_3CH_2-	-	Vermillion red	>200	75	TiO_2	671s
TiO (HNP-OPD-HAP)	N2	CH_3-	-	Vermillion red	>200	72	TiO_2	671s
TiO (HNP-OPD-BA)	N3	CH_3-	C_6H_5-	Dark brown	>200	75	TiO_2	671s
TiO (HNP-OPD-AA)	N4	CH_3-	CH_3-	Vermillion red	>200	70	TiO_2	671s
TiO (HNP-OPD-EAA)	N5	CH_3-	C_2H_5O-	Vermillion red	>200	72	TiO_2	671s

Figure 1. Synthesis of TiO_2 nanoparticles from [TiOL].

They are also applied for the investigation of degradation capacity of industrial waste samples. In addition, the biological activity of the prepared metal oxide nanoparticles has been studied as well.

2. Experiment

2.1. Chemicals and solvents

Titanyl acetylacetonate (purity 98.9%), acetone (95%), beef extract, peptone, 95% ethanol (purity 95%), potato, dextrose, agar, NaCl, mordent brown 48, *o*-phenylene diamine (OPD), 2-hydroxy-1-naphthaldehyde (HNP), 2-hydroxyaceto phenone (HAP), benzoyl acetone (BA), acetylacetone (AA) and ethyl acetoacetate (EA) were obtained from Merck and Aldrich.

2.2. Synthesis of Schiff base ligands and Ti-complexes

2.2.1. Synthesis of 2-hydroxy-1-naphthaldehyde-o-phenylenediamine (HNP-OPD)

The tridentate mono-Schiff bases of diamine have been prepared by the usual condensation of *o*-phenylenediamine (OPD) with 2-hydroxy-1-naphthaldehyde [18]. *o*-Phenylene diamine (5.41 g, 50 mmol) was dissolved in 50 mL of rectified spirit (RS). To which 2-hydroxy-1-naphthaldehyde (8.61 g, 50 mmol) was added slowly (1:1) with continuous stirring in a round bottom flask. The mixture was heated at 65-68 °C, refluxed for 3 hours and then cooled at room temperature. The product was filtered off, washed with small amount of RS, then dried, and preserved in the desiccator over silica gel along with calcium chloride. Yield: 85%.

2.2.2 Synthesis of asymmetric bis-Schiff base ligands

10 mmol of 2-hydroxy-1-naphthaldehyde-o-phenylenedi amine (HNP-OPD) was dissolved in 30 mL of rectified spirit (RS). To which 10 mmol of 2-hydroxyacetophenone, 2-hydroxy propeophenone (HPP), benzoyl acetone (BA), acetyl acetone or ethyl acetoacetate was added drop wise (1:1) with the continuous stirring in a round bottom flask fitted with a reflux condenser [18]. The mixture was heated at 65-68 °C to reflux for 3 hours and then cooled at room temperature. The product was filtered off, washed with small amount of RS, then dried, and preserved in the desiccator over silica gel along with calcium chloride. Prepared ligands are designed as HNP-OPD-HAP, HNP-OPD-HPP, HNP-OPD-BA, HNP-OPD-AA and HNP-OPD-EA (Figure 1, Table 1), Yield: 80-85%.

2.2.3. Preparation of Schiff base Ti-complexes

Titanyl acetylacetonate (5 mmol, $TiC_{10}H_{14}O_5$) and *bis*-ligands (5 mmol) were dissolved in RS (25 mL) in a separate beaker. Ligand solution was added drop wise with continuous stirring in the solution of titanyl acetylacetonate at room temperature. The reaction mixture was heated to reflux for 3 hours when a colored precipitate was found. After completion of reflux, the dense mixture was transferred in a 100 mL beaker in hot and allowed to be cooled at room temperature. Then the product was filtered off, washed with small amount of RS, dried and preserved in the desiccator over silica gel along with calcium chloride. Yield: 70-75%.

2.3. Synthesis of TiO$_2$ nanoparticles

TiO_2 nanoparticle was prepared by the aerosol method in a furnace based on evaporation-condensation technique. The titanium complexes were loaded into a silicon crucible and then it was placed in a muffle furnace and heated at a rate of 10 °C /min up to 500 °C after 3 hours of heating. Nanoparticles of TiO_2 obtained were allowed to cool. After that, they are collected from the crucible and the final products were washed with ethanol for at least three times to remove impurities and then dried at room temperature. Finally, the prepared metal oxide nanoparticles were stored in a vacuum tube. Figure 1 shows the synthesis of TiO_2 nanoparticles from [TiOL]. Yield: 95%.

2.4. Characterization

Complexes were characterized on the basis of FT-IR, NMR, and Mass spectra by authors previously [18]. The formation of TiO₂ nanoparticles was checked by X-ray diffraction (XRD) technique using an X-ray diffractometer (Philips Panalytical X'PERT-PRO) which gives the idea about the crystal phase. Fourier transform-infrared measurements (FT-IR) were recorded on KBr pellets with a Prestige-21 FTIR (Shimadzu) spectrophotometer. FE-SEM micrograph of TiO₂ was obtained using JEOL JSM 7600F Field-emission scanning electron microscope which provides information about the particle size and morphology. Elemental analysis was done using energy-dispersive X-ray spectroscopy (EDS) with an EDS attachment on a LEO 1455 UP scanning electron microscope.

2.5. Antimicrobial study

The antibacterial and antifungal activities of the prepared metal oxide nanoparticles were studied against two pathogenic bacteria, *Escherichia coli* and *Bacillus cereus* and three pathogenic fungi, *Aspergillus flavus*, *Rhizopus* and *Fusarium* obtained from Microbiology Department, University of Chittagong, Bangladesh.

2.5.1. Antibacterial activities

At first, 0.1% suspended solutions were prepared by dissolving 0.01 g solid samples in 10 mL DMSO. Secondly, a small amount of both microorganisms was taken into two different test tubes containing nutrient broth which was prepared by mixing peptone, beef extract, NaCl, and DW and then incubated for 3 h at 37 °C. On the other hand, 10 mL of nutrient broth were transferred in some test tubes, which were capped and placed in an autoclave for 20 min at 121 °C. After that, with the help of micropipette 100 microliters of the prepared sample solutions were further added to this sterilized nutrient broth. Then, 100 microliters of incubated microorganisms were also inoculated with these. Finally, the test tubes were incubated at 37 °C for a specific time duration and the absorbance of the solution was recorded by UV-Spectrophotometer at 625 nm [19].

2.5.2. Antifungal activities

At the beginning, 0.1% solutions were prepared by dissolving 0.01 g solid samples in 10 mL DMSO. Secondly, 25 mL of potato dextrose liquid media [19,20] was taken in some conical flasks. This medium was prepared by mixing potato extract, dextrose, and distilled water. These flasks were capped and sterilized at 121 °C for 20 min. After that, with the help of a micropipette, 100 microliter suspended sample solutions were added to these sterilized liquid media. Finally, the microorganism was transferred to those conical flasks by a loop and then shaken well. Similarly, the same number of solutions was prepared without mixing the microorganism. The pH of all solutions was measured and recorded as initial pH, then placed them in the incubator for 5 days at 27 °C. After 5 days of incubation, all solutions were filtered and collected not only the filtrate solution for pH measurement by pH meter but also the organism for biomass (weight) measurement after drying in an oven at 60 °C.

2.6. Photo-catalytic activity of TiO₂ nanoparticles

2.6.1. Test dye

In the present study, to highlight the photocatalytic activity of TiO₂ nanoparticles, a solution of Mordant Brown 48 (Sigma Aldrich) of certain concentration was used as the standard dye.

Two other dye solutions as waste were collected from two dying industries located in Chittagong.

2.6.2. Selection of λ_max of dyes

A small amount of solid Mordant Brown 48 was taken by a spatula in a conical flask containing 300 mL of distilled water and mixed it homogenously. For better mixing, the solution was placed in the orbital shaker and shook the solution at 200 rpm for 5 minutes. This solution is the mother liquor of unknown concentration. The λ_{max} (The wavelength of maximum absorbance) and the absorbance at λ_{max} of the solution were measured by UV visible spectrophotometer and recorded. λ_{max} for Mordant Brown 48 = 492 nm. Again, a small volume of two industrial dye solutions were taken in two different beakers and diluted to a certain factor with distilled water and shook properly by the help of an orbital shaker. The λ_{max} and the absorbance at λ_{max} of the two solutions were measured by UV visible spectrophotometer and recorded.

2.6.3. Removal efficiency

Five conical flasks of 100 mL were taken and labelled as N1, N2, N3, N4, and N5. 50 mL of the dye solution was taken in each conical flask and the absorbance was measured. And then, 0.0025 g of prepared nanoparticles was added in each flask. Suspended solutions were formed and then they were kept in the dark and shaken in the orbital shaker simultaneously for 30 minutes and the absorbance was measured. After then, the conical flasks were placed in sun light 30 minutes. Absorbances of those solutions were measured by UV visible spectro-photometer at λ_{max} and recorded. Again, all solutions were shaken in the presence of sun light at 200 rpm in the orbital shaker and the absorbance was measured after every 30 minutes interval up to 240 minutes. Data were recorded and absorbance was plotted against time. Again, the removal efficiency was determined by computing the percentage adsorption using the formula in Equation (1).

$$\% \text{ Adsorption} = \frac{(A_0 - A_e)}{A_0} \times 100 \qquad (1)$$

Here, A_0 represents the initial absorbance of the solution and A_e represents the final (after a certain time) absorbance of that solution.

3. Results and discussion

3.1. Characterization of ligands and complexes

TiO₂ nanoparticles have been synthesized from [TiOL] as a precursor and characterized. Ligands have the potential to act as binegative tetradentate ligands in forming TiOL complexes with a square pyramidal geometry. From the IR spectra it is seen that the bands observed between 1640 to 1675 cm⁻¹ for the free ligands were due to the νC=N of the azomethine group [18]. Negative shifting of which indicates the complex formation [18,19]. The presence of νOH in the ligands is indicated by the bands observed at 3350-3400 cm⁻¹, which is further confirmed by the presence O-H signal at δ 12.05 ppm in the ¹H NMR spectra of the ligand [19]. Mass spectrum evidence of the ligands and complexes and their fragmentation pattern also confirms their formation [18]. Absence of νOH bands in both IR and ¹H NMR spectra is a good agreement for the complex formation [19]. In addition, the IR peak at 420-470 cm⁻¹ due to νTi-O indicates the ligand-to metal bonds. The physical properties of the prepared Schiff base complexes as used for TiO₂ nanoparticle synthesis, their identification, and characteristic infrared frequencies (cm⁻¹) have been given in Table 1.

Table 2. XRD analysis report of TiO₂ nanoparticles from TiO (HNP-OPD-HPP).

Position [2θ, °]	Height [cts]	Full width at half maximum [2θ, °]	d-spacing [Å]	Relative intensity [%]
25.5760	198.72	0.3936	3.48297	100.00
27.7172	108.40	0.2755	3.21858	54.55
36.3428	51.75	0.1968	2.47205	26.04
38.1753	37.92	0.4723	2.35750	19.08
41.5280	28.63	0.2362	2.17460	14.41
44.3095	8.63	0.4723	2.04433	4.34
48.3716	68.67	0.3149	1.88172	34.55
54.6196	87.49	0.3149	1.68033	44.03
55.3804	42.15	0.3149	1.65903	21.21
56.9000	23.03	0.3149	1.61828	11.59
63.0186	36.99	0.4723	1.47509	18.62
69.2674	21.66	0.6720	1.35538	10.90

3.2. Characterization of TiO₂ nanoparticles

3.2.1. Physical properties of TiO₂ nanoparticles

All prepared nanoparticles are white colored. The melting points of nanoparticles were very high. All nanoparticles were quite stable at room temperature and can be stored for a long time. The nanoparticles were insoluble in water, acid, and organic solvents like DMSO and DMF. For antimicrobial study suspended solution of nanoparticles was used. TiO₂ nanoparticles were further characterized on the basis of magnetic properties, FTIR, XRD, EDS and SEM analysis.

3.2.2. Magnetic property analysis

Magnetic properties of TiO₂ NPs were carried out using a magnetometer at room temperature. The behavior of a compound in a magnetic field is either being diamagnetic, paramagnetic, or ferromagnetic. Titanium which contains two electrons in 3d-orbital exists in three common oxidation states like Ti(II), Ti(III), and Ti(IV). In Ti(IV), no unpaired electron exists in the 3d orbital. As a result, it has no ability to show paramagnetic behavior rather diamagnetic. TiO₂ nanoparticles showed diamagnetic character which are not attracted by the applied magnetic field. It was confirmed through magnetic susceptibility calculation. Magnetic susceptibility of TiO₂ (N2 and N3) was found a negative value that confirms the diamagnetic character and because the negative value of magnetic susceptibility indicates the diamagnetic nature. As a result, the electronic configuration and magnetic susceptibility calculation support the existence of Ti^{4+}.

3.2.3. Infrared spectra

Infrared spectroscopy involves the interaction of infrared radiation with matter. A substance can be determined by the absorbance bands that are observed in the FT-IR spectrum. A broad band appears in between 880 and 380 cm^{-1} for TiO₂ when sample heating at 300-500 °C [20]. In the infrared spectra of the nanoparticles, the intense peak at the range of 671-690 cm^{-1} is characteristic to Ti-O bending mode of vibration, which confirms to have the Ti-O bond in TiO₂ nanoparticles. And there are no other bands except 2330 and 2360 cm^{-1} which are due to CO_2.

3.2.4. X-ray diffraction

X-ray diffraction (XRD) is a rapid and one of the most powerful scientific analytical techniques primarily used for phase identifying and quantifying various kinds of crystalline materials [11-13] and it can provide information on unit cell dimensions. All the compounds generally show a number of peaks in XRD (2θ°) spectrum, the XRD peaks give an idea about the identity of the substances. TiO₂ is most likely to be a mixture rather than pure anatase and rutile, both of which are well-known as stable phases of titanium dioxide (TiO₂), identified by

XRD [16]. Furthermore, the control of the transformation between anatase and rutile is one of the most important issues in synthesis [17]. XRD is an established nondestructive method for qualitative and quantitative analysis of the phase composition of TiO₂ [21]. Usually TiO₂ in the anatase form gives peaks at 25, 38, 48, 53, 55, 63, 70° and so on at 2θ values [22]. And in the rutile form, TiO₂ gives peaks of at 27, 36, 41, 54, 56, 64, 69° and so on 2θ values [23]. The X-ray diffraction patterns of the synthesized TiO₂ nanoparticles are shown in Figure 2 and the values for TiO (HNP-OPD-HPP) are given in Table 2. The experimental XRD pattern agrees with the JCPDS card no. 21-1272 (anatase TiO₂) and the XRD pattern of TiO₂ nanoparticles from other literature [24]. Here is a sharp peak at 25°, the intensity of which is 100, and there are also some other peaks in 38, 48, 53, 55, 63, and 69° at 2θ value. The peak 25° at 2θ value confirms the TiO₂ anatase structure [25]. Strong diffraction peaks at 25 and 48° indicate TiO₂ in the anatase phase [26,27]. There is no any spurious diffraction peak found in the sample. The intensity of XRD peaks of the sample reflects that the formed nanoparticles are crystalline and broad diffraction peaks indicate very small size crystallites.

3.2.5. Scanning electron microscope

Scanning electron microscope (SEM) is not only capturing the images of the objects and but also can give the idea about the size of the objects. The SEM is routinely used to generate high-resolution images of the shapes of objects. The SEM is also widely used to identify phases based on qualitative chemical analysis and/or crystalline structure. Scanning electron microscope (SEM) was used for the morphological study of nanoparticles of TiO₂. Figure 3 shows the SEM images of the TiO₂ nanoparticles prepared by calcination of titanium complexes at 500 °C for 3 hours from. The TiO₂ nanoparticles formed were agglomerated or coagulated. The nanoparticles seen by SEM images consist of a number of crystallites. From the SEM, it can also be confirmed that the size of the prepared particles is in the nano-range (1-100 nm) and the average dimension of TiO₂ nanoparticles is 30-40 nm and the shape of the particles is visible through the SEM analysis.

3.2.6. Energy-dispersive X-ray spectroscopy

For chemical characterization or elemental analysis, Energy-Dispersive X-ray spectroscopy is a very effective analytical technique. EDS can be used to determine which chemical elements are present in a sample and can be used to estimate their relative abundance. The spectrum of Energy-Dispersive X-ray spectroscopy in Figure 4 is the evidence of the presence of only titanium and oxygen in that molecule. On the other hand, XRD result also proved that this molecule is titanium dioxide. The EDS pattern of samples showed the presence of TiO₂ nanoparticles which were produced by direct calcination method using titanium complexes of Schiff bases as a precursor. Hence, it is proved that the prepared nanoparticles contain only titanium and oxygen in the form of TiO₂.
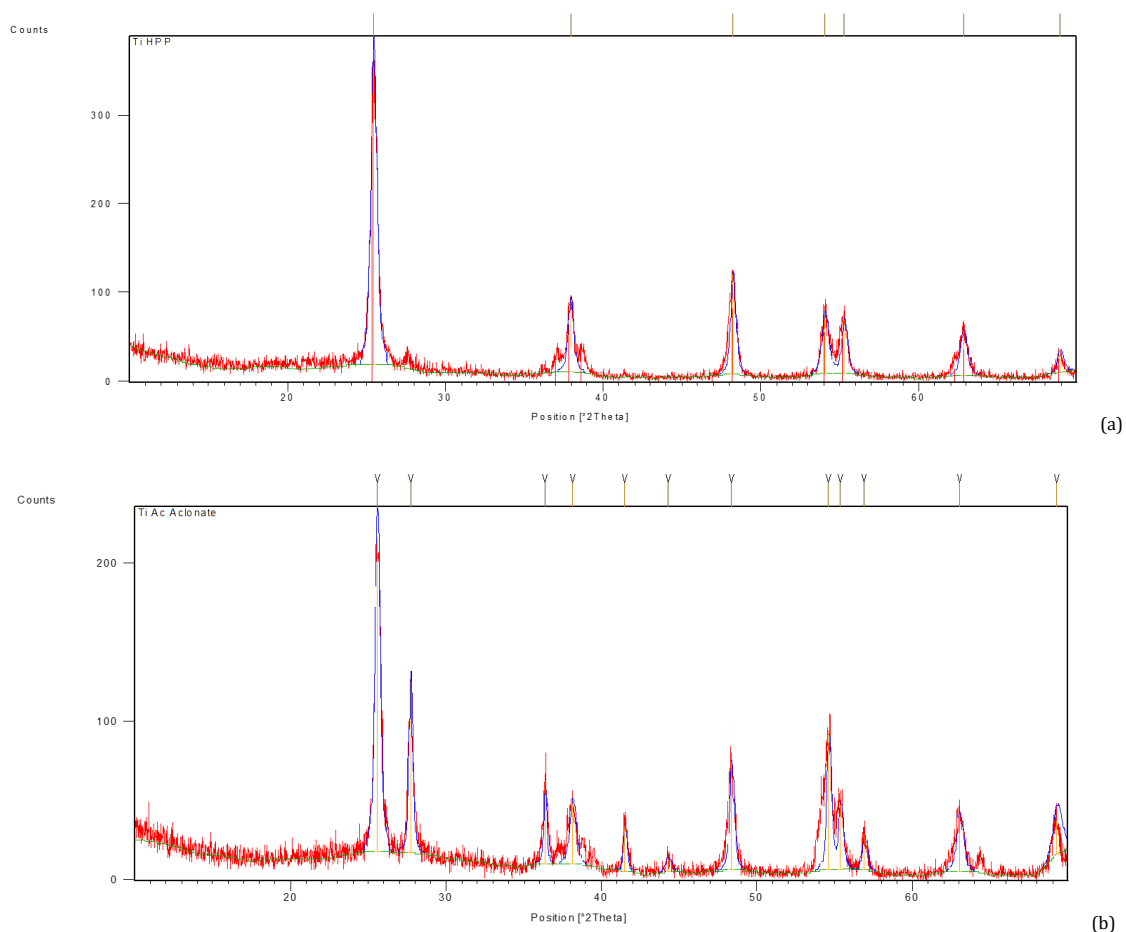
Figure 2. XRD of TiO₂ nanoparticles (a) N1 from TiO(HNP-OPD-HPP) and (b) N5 from TiO(HNP-OPD-EAA).
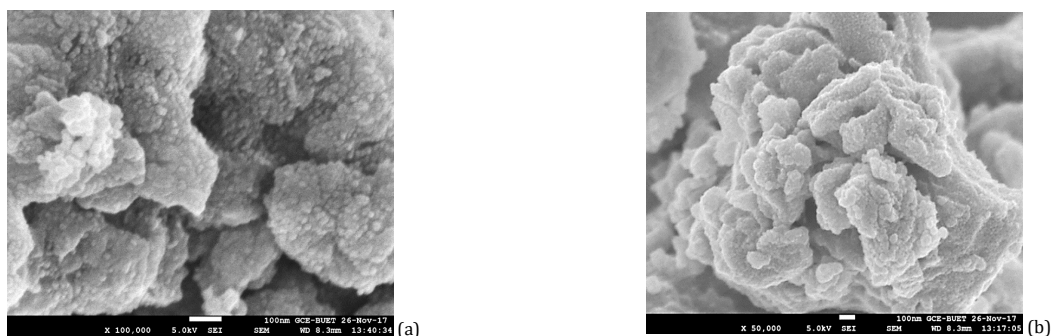

Figure 3. SEM of TiO₂ nanoparticles prepared from (a) [TiO(HNP-OPD-HAP)] and (b) [TiO(HNP-OPD-HPP)] (Resolution × 50,000).

TiO₂ nanoparticles have been synthesized from [TiOL] as a precursor and characterized. In the infrared spectra of the nanoparticles, the band at the range of 671 cm^{-1} is characteristic to Ti-O bending mode of vibration, which confirms to have the Ti-O bond. XRD analysis confirmed that the synthesized nanoparticles are TiO₂ in the anatase form as the XRD shows peaks in 25, 38, 48, 53, 55, 63, and 69° at 2θ values. From the SEM images of the prepared TiO₂ nanoparticles, it is confirmed that the nanoparticles are agglomerated or coagulated consist of a number of crystallites and the average dimension of nanoparticles is 30-40 nm in diameter which proves that the particles are in the nano-range. The peaks of EDS are the evidence of the presence of titanium and oxygen. The unexpected peak for carbon is coming from the grids that used as a substrate during the EDS analysis. It is also can be proved

from the IR spectra. Finally, it can be said that the prepared substances are titanium dioxide which are in the nano size and are in the anatase form.

3.3. Microbial properties

3.3.1. Antibacterial activities

Through the liquid culture method, antibacterial activities were checked by measuring the absorbance by spectrophotometer at 625 nm. Figure 5 represents the antibacterial activity of the prepared nanoparticles against tested bacteria. After 15 to 24 hours incubation in the presence of the prepared nanoparticles, the growth of the bacteria was evaluated.
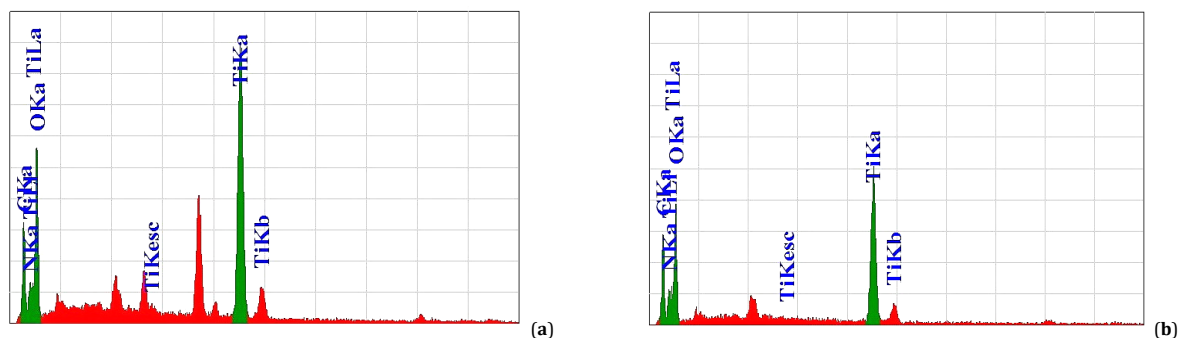
Figure 4. EDS of TiO₂ nanoparticles from (a) TiO(HNP-OPD-EAA) and (b). TiO(HNP-OPD-HPP).
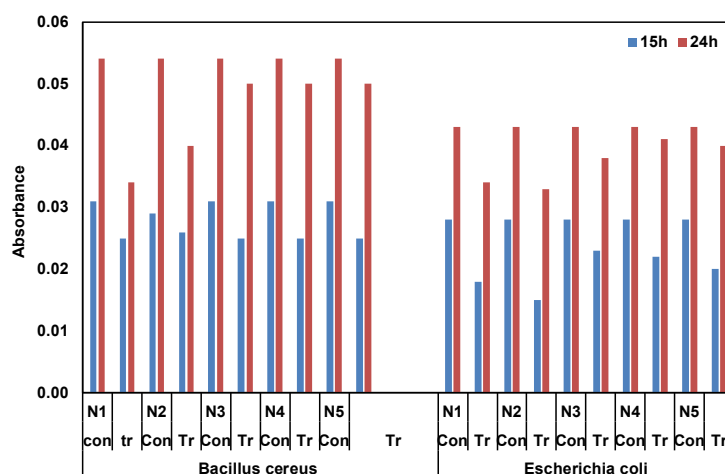

Figure 5. Antibacterial activities of prepared nanoparticles against tested bacteria (Con = Control, Tr = Treatment).

Figure 5 is the represents bacterial activity for all prepared nanoparticles against *Bacillus cereus* and *Escherichia coli*. Here, N1 and N2 were showing higher activity but N3, N4, and N5 were showing less activity against *Bacillus cereus* after 24 hours. Similarly, against *Escherichia coli* again N1 and N2 were showing higher activity and N3, N4, and N5 were showing less activity after 24 hours. Finally, from the graphs it is clear that the growth of bacteria in all sample solutions was lower than the growth of bacteria in control (without sample). This indicates that the prepared nanoparticles are showing inhibiting activity rather than inducing activity against the test organisms.

3.3.2. Antifungal activities

The prepared nanoparticles were tested by liquid media method by measuring the biomass (weight) and pH of the solutions against *Aspergillus flavus, Rhizopus*, and *Fusarium*. Figure 6 shows the biomass data of the prepared nano particles against those fungus species. In the control of *Rhizopus, Fusarium, Aspergillus flavus* species pH became acidic (after 5 days). Here, in the presence of nanoparticles, the *Rhizopus* medium became acidic, i.e., the pH of the samples N1, N3, N4 became less than that of control and the pH of the sample N2, N5 are as same as the control. The weight of biomass was less in the test sample N2, N3, N4 from that of Fusarium control, but N1 and N2 had higher biomass. From this, it is seen that N1 and N5 have the inducing capacity, whereas N2, N3, N4 have inhibiting capacity. Again, in the presence of nanoparticles the *Fusarium* medium also became a little more acidic, i.e., the pH of all samples became less than that of control. The weight of biomass was less in the test sample from that of *Fusarium*

control except N1. Hence, it is seen that only N1 has the inducing capacity, whereas N2, N3, N4, N5 have inhibiting capacity. Similarly, in the presence of nanoparticles, the *Aspergillus flavus* medium became acidic, i.e., the pH of the samples N1, N3, N5 became higher than that of control and the pH of the sample N4 were as same as the control and N2 has less. The weight of biomass was less in the test sample from that of *Aspergillus flavus* control except N4. Therefore, it is seen that only N4 has the inducing capacity whereas other samples have inhibiting capacity. All the results indicated that the nanoparticles have the tendency to decrease the microbial biomass of the selected species.

3.4. Photo-catalytic activity

The photocatalytic experiment was conducted in an atmospheric system. The experimental data was collected in two ways to confirm the photocatalytic activities such as catalytic and photolytic. Photolytic (sun light) degradation of Mordent Brown 48 (MB) was done in absence of TiO₂ nanoparticles. The absorbance of the solution was found to be almost same, indicating zero degradation.

Catalytic degradation was carried out using TiO₂ nanoparticles both in the absence and in the presence of light to compare the results. It has been seen that the initial absorbance was 0.222 at 492 nm (λ_{max}) for Mordent Brown 48 which was decreased gradually after the time interval. It was seen that in the absence of light only 8.18% degradation was occurred by the time of 240 min. Figure 7 shows that after 180 min the degradation gained a constant value. It was clear from the differences observed between the first FTIR spectra and FTIR spectra taken without light. It was caused due to the adsorption
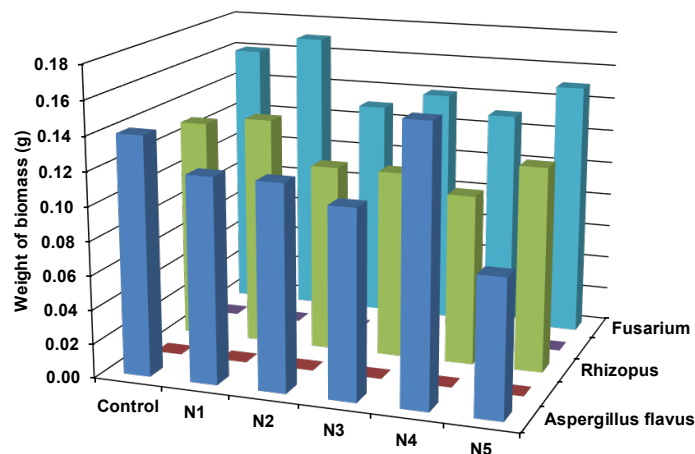
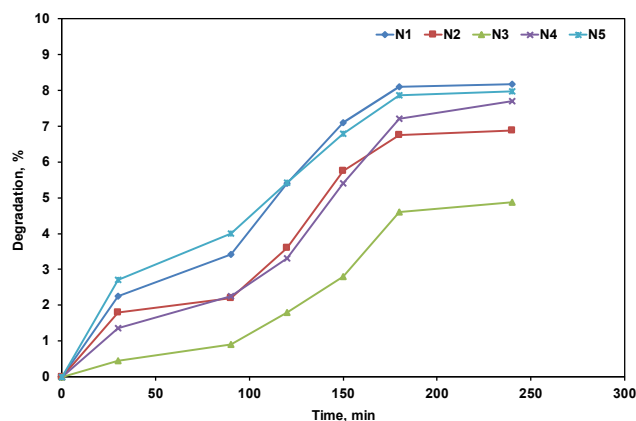**Figure 6.** The biomass data of antifungal activity of prepared nanoparticles.

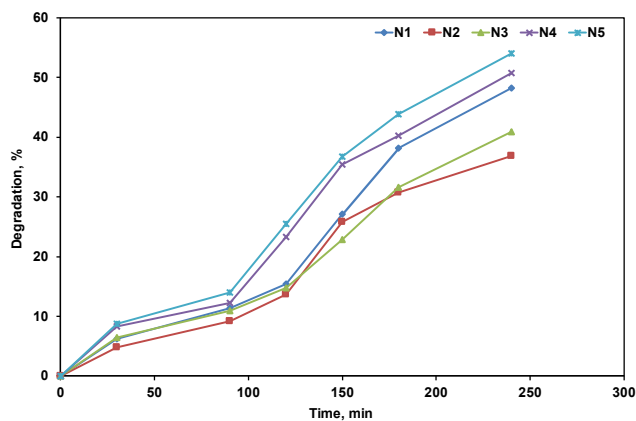**Figure 7.** Degradation (%) of MB in the presence of light.

Figure 8. Degradation (%) of MB in presence of TiO$_2$ NPs and light.

of Mordent Brown 48 dye on TiO$_2$ nanoparticles. However, quite different spectrum of Mordent Brown 48 dye was obtained when the similar experiment was done in the presence of light as shown in Figure 8. However, in presence of light, a considerable amount (maximum 53.98%) of dye was degraded by TiO$_2$ nanoparticles [26]. It is because there are many functional groups and bonds that have been destroyed. These results concluded that TiO$_2$ nanoparticles showed good catalytic activity against Mordent Brown 48. Here N5 shows the highest and N2 shows the lowest % of degradation in Mordent brown 48.

For industrial dye solutions, the absorbances were 0.137 at 582 nm (λ_{max}) and 0.087 at 506 nm, respectively, which were also gradually decreased with the increase of time. Figure 9 represents the % of degradation of two industrial dye solutions catalysed by the prepared nanoparticles. N3 shows the highest (18.23%) and N2 shows the lowest (14.32%) degradation for Industrial dye solution 1. Figure 10 shows that N3 has the highest (54.03%) and N2 has the lowest (33.35%) degradation for Industrial dye solution 2.
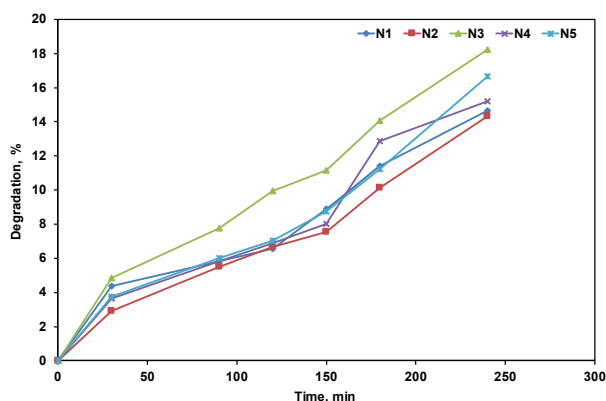
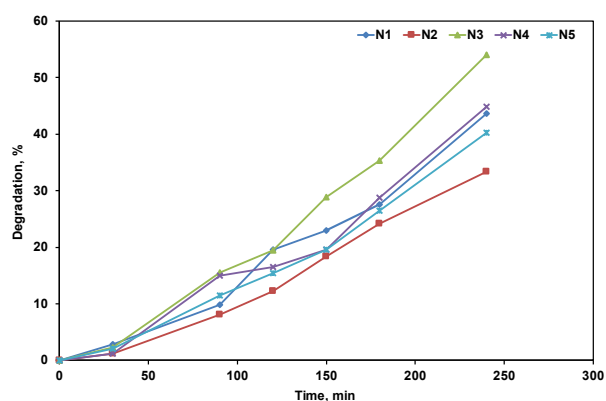**Figure 9.** Degradation (%) of industrial sample 1 in the presence of TiO_2 NPs and light.

Figure 10. Degradation (%) of industrial sample 2 in the presence of TiO_2 NPs and light.

4. Conclusion

The present work focused on the synthesis, characterization, and applications of titanium dioxide nanoparticles when Ti(IV)-complexes of Schiff bases were used as a precursor. The IR spectrum showed a peak at 671 cm^{-1} which provides the information about the presence of a metal-oxygen bond, that is titanium-oxygen bond. In XRD spectrum, there are peaks at 25, 38, 48, 53, 55, 63, and 69° at 2θ value which proved that the compound is TiO_2 in the anatase form. The existence of only titanium and oxygen elements are confirmed by EDS. SEM provides the particle size from which it is confirmed that the prepared nanoparticles have a diameter of 30-40 nm approximately and shows that the nanoparticles were aggregated and formed a cluster of TiO_2. From the catalytic study, it is clear that organic dyes were degradated up to 54.0 % by the prepared TiO_2 nanoparticles; hence they can be used for the industrial waste water treatment. Prepared TiO_2 nanoparticles also showed considerable inhibition capacity on the growth against selected plant pathogenic fungi i.e., *Aspergillus flavus, Rhizopus*, *Fusarium* and human pathogenic bacteria i.e. *Escherichia coli*, *Bacillus cereus.*

Acknowledgements

Disclosure statement DS

Conflict of interests: The authors declare that they have no conflict of interest.

Author contributions: All authors contributed equally to this work.
Ethical approval: All ethical guidelines have been adhered.
Sample availability: Samples of the compounds are available from the author.

ORCID iD

Mohammad Nasir Uddin
iD https://orcid.org/0000-0003-1235-2081
Tareq Mahmud
iD https://orcid.org/0000-0002-4244-6356
Wahhida Shumi
iD https://orcid.org/0000-0001-7593-6792
AKM Atique Ullah
iD https://orcid.org/0000-0002-4545-2663

References

[1]. Lawrence J. F.; Frei R. W. Chemical Derivatization in Chromatography, Elsevier, Amsterdam, 1976.
[2]. Zaki, Z. M.; Haggag, S. S.; Soayed, A. A. *Spectrosc. Lett.* **1998**, *31*, 757–766.
[3]. Shama, S. A.; Omara, H. *Spectrosc. Lett.* **2001**, *34*, 49–56.
[4]. Gaballa, A. S.; Asker, M. S.; Barakat, A. S.; Teleb, S. M. *Spectrochim. Acta A Mol. Biomol. Spectrosc.* **2007**, *67*, 114–121.
[5]. da Silva, C. M.; da Silva, D. L.; Modolo, L. V.; Alves, R. B.; de Resende, M. A.; Martins, C. V. B.; de Fatima, A. *J. Adv. Res.* **2011**, *2*, 1–8.
[6]. Uddin, M. N.; Ahmed, S. S.; Alam, S. M. R. *J. Coord. Chem.* **2020**, *73* (23), 3109–3149.
[7]. Saghatforoush, L. A.; Mehdizadeh, R.; Chalabian, F. *J. Chem. Pharm. Res.* **2011**, *3*(2), 691-702.
[8]. Sheikhshoaie I.; Ranjbar Z. R.; Sohaleh H. *Chem. Xpress.* **2014**, *3*(4), 167-172.
[9]. Mazzola, L. *Nat. Biotechnol.* **2003**, *21*, 1137–1143.
[10]. Paull, R.; Wolfe, J.; Hébert, P.; Sinkula, M. *Nat. Biotechnol.* **2003**, *21*, 1144–1147.

[11]. Khalaji D.; Rahdari A. R. *Int. J. Bio-Inorg. Hybrid Nanomater.* **2015**, *4* (4), 209–213.

[12]. Abdel-Rahman, L. H.; Abu-Dief, A. M.; Newair, E. F.; Hamdan, S. K. *J. Photochem. Photobiol. B* **2016**, *160*, 18–31.

[13]. Kessler, R. *Environ. Health Perspect.* **2011**, *119*, a120-5.

[14]. Zhang, Y.; Leu, Y.-R.; Aitken, R. J.; Riediker, M. *Int. J. Environ. Res. Public Health* **2015**, *12*, 8717–8743.

[15]. Petković, J.; Zegura, B.; Stevanović, M.; Drnovšek, N.; Uskoković, D.; Novak, S.; Filipič, M. *Nanotoxicology* **2011**, *5*, 341–353.

[16]. Farbod, M.; Khademalrasool, M. *Powder Technol.* **2011**, *214*, 344–348.

[17]. Sugimoto, T.; Zhou, X.; Muramatsu, A. *J. Colloid Interface Sci.* **2002**, *252*, 339–346.

[18]. Uddin, M. N.; Siddique, Z. A.; Mase, N.; Uzzaman, M.; Shumi, W. *Appl. Organomet. Chem.* **2019**, *33*, e4876.

[19]. Uddin, M. N.; Khandaker, S.; Moniruzzaman; Amin, M. S.; Shumi, W.; Rahman, M. A.; Rahman, S. M. *J. Mol. Struct.* **2018**, *1166*, 79–90.

[20]. Uddin, M. N.; Chowdhury, D. A.; Mase, N.; Rashid, M. F.; Uzzaman, M.; Ahsan, A.; Shah, N. M. *J. Coord. Chem.* **2018**, *71*, 3874–3892.

[21]. Jensen, H.; Soloviev, A.; Li, Z.; Søgaard, E. G. *Appl. Surf. Sci.* **2005**, *246*, 239–249.

[22]. Jenkins R.; Snyder R. L., Introduction to X-Ray Powder Diffractometry; John Wiley & Sons: London, 1996.

[23]. Pinjari, D. V.; Prasad, K.; Gogate, P. R.; Mhaske, S. T.; Pandit, A. B. *Ultrason. Sonochem.* **2015**, *23*, 185–191.

[24]. Czanderna, A. W.; Rao, C. N. R.; Honig, J. M. *Trans. Faraday Soc.* **1958**, *54*, 1069–1073.

[25]. Swanson H. E.; Tatge E. *Natl. Bur. Std. U.S. Circ.* **1953**, *539*, 46-47.

[26]. Ba-Abbad, M. M.; Kadhum, A. A. H.; Mohamad, A. B.; Takriff, M. S.; Sopian, K. *Int. J. Electrochem. Sci.* **2012**, *7*, 4871-4888.

[27]. Uddin, M. N.; Rahman, M. S.; Shumi, W.; Hossain, M. K.; Ullah, A. K. M. A. *J. Chem. Sci. (Bangalore)* **2020**, *132*.